

Journal of Materials Chemistry B

Accepted Manuscript



This is an *Accepted Manuscript*, which has been through the Royal Society of Chemistry peer review process and has been accepted for publication.

Accepted Manuscripts are published online shortly after acceptance, before technical editing, formatting and proof reading. Using this free service, authors can make their results available to the community, in citable form, before we publish the edited article. We will replace this *Accepted Manuscript* with the edited and formatted *Advance Article* as soon as it is available.

You can find more information about *Accepted Manuscripts* in the [Information for Authors](#).

Please note that technical editing may introduce minor changes to the text and/or graphics, which may alter content. The journal's standard [Terms & Conditions](#) and the [Ethical guidelines](#) still apply. In no event shall the Royal Society of Chemistry be held responsible for any errors or omissions in this *Accepted Manuscript* or any consequences arising from the use of any information it contains.

Cite this: DOI: 10.1039/c0xx00000x

ARTICLE TYPE

www.rsc.org/xxxxxx

Calcium-modified microporous starch with potent hemostatic efficiency and excellent degradability for hemorrhage control

Fangping Chen ^{a,b,c}, Xiaoyan Cao ^c, Xiaolong Chen ^c, Jie Wei ^{a,b, c *} and Changsheng Liu ^{a,b,c *}*Received (in XXX, XXX) Xth XXXXXXXXX 20XX, Accepted Xth XXXXXXXXX 20XX*

DOI: 10.1039/b000000x

Effective hemorrhage control is vital for reducing the mortality after major trauma both in citizen life and in military. In recent years, microporous starch (MS) has been used as a hemostatic agent. However, MS has insufficient hemostatic capacity to stop severe bleeding. To improve its hemostatic performance, in this study calcium-modified microporous starch (CaMS) was firstly developed *via* oxidization and self-assembling with calcium ions (Ca²⁺) on MS, and the hemostasis efficiency and degradation behaviour were evaluated. The results showed that carboxyl groups and Ca²⁺ had been modified successfully onto the MS. MS and CaMS both engaged the hemostatic response by rapid absorption and swelling due to porous structure and high surface area. It was noteworthy that CaMS activated an intrinsic pathway of coagulation cascade and induced platelets adherence because of the modified Ca²⁺ and carboxyl groups. The synergistic effects of chemical activation mechanism and physical absorption mechanism resulted in a dramatic improvement in the hemostatic capacity of CaMS, and thus achieved an effective hemorrhage control in rabbit liver and femoral artery injury. Additionally, the degradation of CaMS was improved greatly by modification. In conclusion, CaMS effectively improved the hemostatic performance and degradability. CaMS would be a promising material for designing hemostatic in more extensive clinical application.

Introduction

Uncontrolled hemorrhage from trauma is a leading cause of death both in citizen life and in military.^{1,2} Effective control of blood loss is of great significance for improved survival and a reduction in delayed causes of death from resultant coagulopathy, infection, and multisystem organ failure.³⁻⁵

As a complement to traditional surgical techniques, biomaterials have been developed for control life-threatening extremity hemorrhage.⁶⁻⁹ Although some have proved valuable for hemorrhage control in many cases, and even some (HemCon[®] and QuickClot[®]) are currently available in the market, their main limitations are lack of efficacy in severe bleeding. For example, HemCon[®] dressing pads are difficult to apply over complex

sites due to their rigidity. Additionally, the inconsistent performance of HemCon[®] was another issue owing to batch-to-batch variation.¹⁰ QuickClot[®] is not degradable and needs to be removed, so it can only be used in external hemorrhages¹¹, and tissue damage was reported due to the heat released during the application of QuickClot[®] as well.¹² Hence, the development of an alternative effective hemostatic that can control the bleeding and minimize collateral damage is still an enormous challenge.

Due to high porosity, huge surface area and extraordinary water imbibition, MS has been considered prominent candidates for many applications, such as a temporary vascular occlusion, drug carriers,¹³ adsorbents, and catalyst carriers.¹⁴ MS spheres (Arista[®], Medafor, USA) were manufactured by cross-linking starch with epichlorohydrin to form glycerol-ether links (1-3 dioxopropanol). Since 2002, Arista[®] has been approved by FDA and used clinically as a topical hemostatic agent. Arista[®] facilitates hemostasis because it absorbs the fluid from the blood and increases the concentration of the endogenous coagulation factors and platelets factors at the site of bleeding, thus forming blood clots.¹⁵ In addition, Arista[®] allows the body's own enzymes to rapidly break the MS up into oligosaccharide, maltose and glucose, and can be finally absorbed by tissue, which allows for internal hemorrhage. Combined with its biosafety in source, simplicity in preparation and a long shelf life in storage, MS has become one of the most attractive hemostatic agents.

^aThe State Key Laboratory of Bioreactor Engineering, East China University of Science and Technology, Shanghai 200237, PR China. Fax: 86-21-64251358; Tel.:86-21-64251308; E-mail: fpchen@ecust.edu.cn; liucs@ecust.edu.cn

^bKey Laboratory for Ultrafine Materials of Ministry of Education, School of Materials Science and Engineering, East China University of Science and Technology, Shanghai 200237, PR China

^cEngineering Research Center for Biomedical Materials of Ministry of Education, East China University of Science and Technology, Shanghai 200237, PR China

[†]Electronic Supplementary Information (ESI) available. See DOI: 10.1039/b000000x/

Although effective in hemorrhage control in low flow bleedings,¹⁵⁻¹⁶ MS has shown insufficient hemostatic capacity to stop larger and severe bleeds.¹⁷⁻²⁰ When combined with recombinant factor VIIa, evidence was found of an increased hemostatic effect.¹⁸ However, MS is still insufficient to stem the larger bleeds.²¹ It is well accepted that hemostatic materials can be divided into passive or active hemostatic agents or combinations thereof.²² Only active hemostatic agents can stop larger bleeds, which activate the blood coagulation system and accelerate the fibrin formation process, thereby facilitating the rapid creation of a strong hemostatic clot.²² However, MS merely relies on rapid absorption and swelling to achieve a hemostasis. It falls in the category of passive hemostatic agents, along with gelatin, collagen, and oxidized cellulose. In addition, neither enhanced coagulation nor platelet activation by MS was found.²³ From this viewpoint, the hemostatic capacity of MS would be enhanced if it activated platelets or triggered coagulation.

Combining active agents, such as fibrinogen or thrombin, with MS is an effective way to improve the interaction with blood and increase the formation and strength of clotting. However, their origin from extraneous human or animals would increase the risk of disease or viral infection, which heavily restricts their clinical application.

Chemically modifying MS is an alternative method to introduce the abilities to activate the blood coagulation system. Björnses et al first proposed the idea and modified MS with N-octenylsuccinic anhydride, chloroacetic acid, acetic anhydride, diethylaminoethyl chloride and ellagic acid. The results showed an ability to activate platelets, resulting in a dramatic improvement in the hemostatic capacity of the modified MS *in vivo*.²³ However, the modified MSs were no longer viable in clinical application due to their toxic modifications or poor degradability. Ideally, to accelerate the healing process and ensure security without any infection, the surplus agents should be biodegradable.²⁴⁻²⁵ Therefore, it is beneficial to develop MSs by chemical modification into more effective, biodegradable, and non-toxic topical hemostatic agents.

Calcium ions (Ca^{2+}) influence the fibrinogen-fibrin transition, shortening the clotting time of fibrinogen by thrombin.²⁶ Our team's result further confirmed that calcium doped mesoporous silica spheres possessed superior hemostatic properties, as compared to pure mesoporous silica spheres.³ Due to a positive effect of Ca^{2+} on the hemostatic effects of mesoporous silica, and the biodegradable nature of MS, it would be prudent to expand research in this area by creating calcium modified MS. Currently there is no existing literature concerning the hemostatic efficacy of calcium modified MS.

The purpose of this study was first to develop a calcium modified microporous starch (CaMS) hemostatic agent via oxidization and self-assembling of MS, and secondly to evaluate the hemostatic efficiency of CaMS both *in vitro* and *in vivo*. Additionally, the degradable behavior of the CaMS was also investigated by immersion in modified simulated body fluid (mSBF).

Experimental

Preparation of 6CaMS and 9CaMS

Native corn was purchased from Jiugui Starch Co., Shanghai, China. Glucoamylase and α -amylase, with activity at least 100,000 U/g, were purchased in liquid from Jiahe Biotechnology Co., Shanghai, China. All other chemicals were of reagent grade and were used as recommended by the manufacturers. The reaction scheme illustration for the CaMS is depicted in Fig. 1. There were three main steps involved in the CaMS preparation:

- 1) MS formed through enzymolysis the corn starch;
- 2) Catalytic oxidation of MS;
- 3) Self-assembling with Ca^{2+} .

1) MS formation by enzymolysis

Corn starch (100 g) was mixed with Na_2HPO_4 -citric acid buffer (20 mL, pH = 5.8) in a 100 mL Erlenmeyer flask and was stirred on a magnetic stirrer. Next glucoamylase and α -amylase (both 0.05% v/v) at volume ratio of 1:4 were then added to the mixture. The resulting starch slurry was stirred at 50 °C for 6 h. At the end of the reaction, 0.1M NaOH was added to stop hydrolysis. The slurry was centrifuged at 4000 rpm for 5 min, vacuum filtered, and washed three times with deionized water, followed by lyophilization 36 h to form 6MS. The preparation of 9MS was same as 6MS except the hydrolysis time was extended to 9 h.

2) Oxidization of MS

6MS or 9MS (30 g) was respectively suspended in 70 mL deionized water in a mechanically stirred glass. CuSO_4 solution (1 mL) as a catalyst and hydrogen peroxide (10 g) as an oxidizer were added dropwise in turn. The oxidation of the mixture lasted 3 h at 45 °C, keeping the pH of 8.0 by addition of 0.5 M NaOH. The resulting materials were then vacuum filtered, washed twice and dried by a freeze dryer for 36 h to yield oxidized microporous starch (6OMS or 9OMS).

3) Self-assembly of OMS

6OMS or 9OMS was self-assembled in the saturated calcium chloride solution for 1 h at 30 °C. The slurries were centrifuged, washed thoroughly with deionized water three times and dried in vacuum-freeze dryer. 6CaMS and 9CaMS were then prepared and stored in a desiccator at room temperature for further analysis. All preparations were made in triplicate.

Characterization of CaMS

The morphology of CaMS was examined through scanning electron microscopy (SEM, JSM-6360LV, JEOL, Japan) coated with gold with an acceleration voltage of 15 kV. The phase compositions were analyzed with X-ray diffraction (XRD, Rigaku, Japan) using $\text{Cu-K}\alpha$ radiation. Fourier-transform infrared spectroscopy (FTIR, Nicolet 380, Thermo, USA) was used to study the structural organization of CaMS.

1) Determination of carboxyl content

The carboxyl content of OMS was determined by alkaline titration. OMS (2 g) was stirred in 30 mL of 0.1 M aqueous HCl for 30 min. The slurry was then filtered and washed with distilled water until free of chlorine ions, which was verified using AgNO_3 solution. The slurry was carefully transferred into a beaker with 300 mL deionized water and heated in a boiling water bath with continuous stirring for 20 min to ensure complete gelatinization.

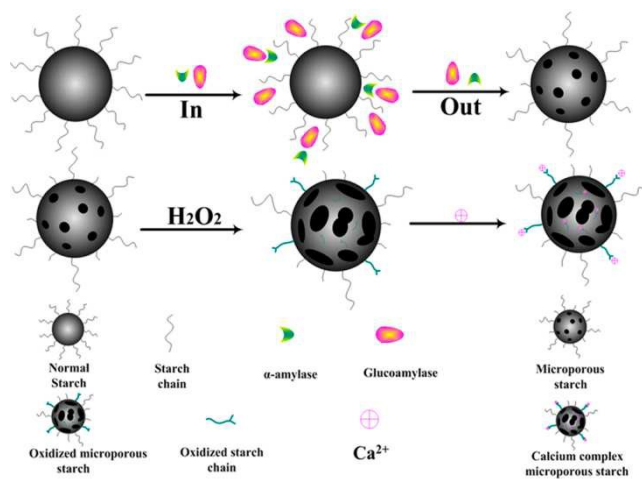


Fig. 1 Reaction scheme illustration for the preparation of CaMS

The hot starch was titrated with 0.1 M NaOH using phenolphthalein as an indicator. A blank determination for MS was carried out in the same manner. In the blank determination the sample had previously been stirred in 30 mL deionized water instead of 0.1 M HCl. The carboxyl content can be calculated according to Equation (1)

$$n = [(V_1 - V_0)/2] \times c \quad \text{Eq. (1)}$$

Where n represents the carboxyl content (mmol); V_1 and V_0 represents the consumption volume of NaOH (mL) for titration of OMS and MS, respectively; and c represents the concentration of NaOH used (mol/L).

2) Calcium content in CaMS

CaMS (1 g) was calcined at 600 °C for 4 h to remove organic compounds. CaCl_2 solution was formed by dissolving the sintered CaMS in 1 M HCl. The Ca^{2+} concentration in the CaCl_2 solution was measured with an inductively coupled plasma-atomic emission spectroscopy (ICP-AES, IRIS 1000, Thermo Elemental, USA).

Degradation in vitro, absorption ratio, solubility and swelling

In vitro degradation was performed by immersing the samples in modified simulated body fluid (mSBF). The degradation rate of the sample was determined by its weight loss rate in the mSBF. Since endogenous levels of α -amylase are approximately 40-220 U/L in human body, mSBF contained 50 mg of 2000 U/g α -amylase and 1 L of pure simulated body fluid (SBF). SBF was prepared according to the procedure described by Kokubo.²⁷ The solution was buffered at pH 7.4 using tris(hydroxymethyl)aminomethane ($(\text{CH}_2\text{OH})_3\text{CNH}_2$) and 1 M HCl at 37 °C.

Before immersion, the samples were dried at 60 °C for 24 h. The initial weight of each sample was accurately measured and recorded as W_0 . The samples were immersed in mSBF at a weight to volume ratio of 0.2 g : 1 mL in plastic bottles. The bottles were continuously shaken in a water bath at 100 rpm in a humidified atmosphere with 5% CO_2 at 37 °C for 7 days, with the solution being changed daily. When the solution was changed, the sample was filtered, gently rinsed with deionized water, and dried at

80 °C to a constant weight. The final weight of each sample was measured and recorded as W_t . The weight loss rate of each sample was calculated according to Equation (2). Each test was repeated three times and the average value was calculated.

$$W\% = [(W_0 - W_t)/W_0] \times 100\% \quad \text{Eq. (2)}$$

The absorption ratio of samples depended on the maximum amount of liquid per unit of materials absorbed in mSBF.^{3, 28} To remove the moisture inside, all samples were vacuum-dried at 80 °C, and then each sample was weighed and recorded as W_0 . After the sample was placed on filter paper in a funnel, and deionized water was continuously added drop-wise to the sample at a rate of 8 mL/min until the sample reached its limit, which was determined when the first drop of fluid fell into the filter flask). The weight of sample at its maximal water absorption was recorded as W_1 . The absorption ratio of each sample can be calculated according to Equation (3)

$$A\% = [(W_1 - W_0)/W_0] \times 100\% \quad \text{Eq. (3)}$$

Cold-water solubility and swelling properties of samples were analyzed in triplicate following the method of Dhital et al.²⁹. In brief, starch samples (200 mg, recorded as W) were suspended in 10 mL distilled water in a tared centrifuge tube. The starch suspension was incubated at 25 °C for 30 min with stirring to extract the cold-water soluble materials. After the suspension was centrifugated at 3000 r / min for 20 min, the supernatant was decanted carefully, dried at 105 °C to a constant weight (A). The residue was also dried and the final weight was recorded as P . Swelling and solubility were determined using the following Equation (4) and Equation (5):

$$\text{Solubility} = A \div W \times 100\% \quad \text{Eq. (4)}$$

$$\text{Swelling rate} = P \div W \times 100\% \quad \text{Eq. (5)}$$

Assessment of plasmatic coagulation in vitro

Activated partial thromboplastin time (APTT) and prothrombin time (PT) were performed using a semi-automatic coagulation analyzer (Biomérieux, France). The study was approved by the Research Center for Drug Safety Evaluation of Shanghai University of Traditional Chinese Medicine. Fresh blood was collected from Sprague-Dawley rats containing 3.8% sodium citrate [sodium citrate : blood = 1 : 9 ($v : v$)] in the siliconized tube. The platelet poor plasma (PPP) was immediately obtained by centrifuging the blood at 3000 rpm for 15 min at 37 °C. APTT: APTT: 6MS or 6CaMS powder was incubated separately with 0.1 mL APTT reagent and 0.1 mL PPP at 37 °C. After incubation for 5 min, 0.1 mL CaCl_2 was added in the test tube and APTT was tested simultaneously. PT: 0.1 mL of PPP was incubated separately with 6MS or 6CaMS powder at 37 °C in test tubes. After incubation for 3 min, 0.2 mL of PT reagent was added and PT was measured simultaneously.

Platelet adhesion

6MS and 6CaMS were used for platelet adhesion measurement. As described in experimental section, 6MS was prepared by enzymolysis from the corn starch with glucoamylase and α -amylase for 6 h. After the 6MS was catalytically oxidized to be 6OMS, Ca^{2+} was self-assembled with 6OMS to form 6CaMS.

Platelet adhesions of 6MS and 6CaMS were determined with a lactate dehydrogenase (LDH) assay. Before the assay, blood from the rabbits' ear-rim vein was mixed with 0.109 M sodium citrate

solution at a ratio of 1:9 in test tubes. Platelet rich plasma (PRP) was obtained by centrifugation at 1500 rpm for 5 min. MS and CaMS granules were incubated at 37 °C for 30 min in PRP with the number of platelets adjusted up to 2×10^8 platelets/mL. Then non-adherent platelets were thoroughly washed by PBS (137 mM NaCl, 2.7 mM KCl, 8 mM $\text{Na}_2\text{HPO}_4 \cdot 12\text{H}_2\text{O}$, 1.5 mM KH_2PO_4) at pH 7.4. Thereafter the samples were placed into a 24-well plate, and the adherent platelets were then lysed with 0.25 mL 1% Triton X-100 in PBS at 37 °C for 1 h. The LDH assay was performed on the lysates using LDH/LD Kit (Sigma-Aldrich, USA) and the number of adherent platelets was determined from the calibration curve. Previously, a calibration curve was obtained in a series of known concentrations of platelets by measuring the OD between 490 nm and 650 nm spectrophotometrically (Multiskan MK3, Thermo Electron Corporation, USA). Standard gauze was used as a control. For each experimental condition, one set of samples ($n=5$) was used for platelet adhesion measurement.

The samples were fixed with 0.1 M phosphate-buffered solution containing 2.5% glutaraldehyde and 2.0% paraformaldehyde (pH 7.4), and then post-fixed with 1% osmium tetroxide in the same buffer. After being dehydrated using a graded series of ethanol solutions, the samples were examined *via* SEM, using the aforementioned experimental parameters.

25 Hemostasis in an animal model

All animal experiments were approved by the ethical committee of the National Tissue Engineer R&D Center (Shanghai, China), and were conducted in accordance with the "Regulations for the administration of affairs concerning experimental animals" issued by the Chinese Ministry of Science and Technology of 31 October 1988.

5-month old male New Zealand White rabbits (wt. 3-4 kg) were purchased from Silaike Co. Ltd (Shanghai, China). They were fasted 24 h with water permitted only. All samples were dried at 80°C in a vacuum oven overnight and then sterilized using ultraviolet radiation (Heming Co. Ltd. Shanghai, China) for 2 h before the experiment. Standard gauze was used as a control. All procedures were performed under sterile conditions.

1) Rabbit liver injury experiment

15 rabbits separated into three groups (6MS, 6CaMS and Standard gauze) were selected for hemostasis in the rabbit liver injury. After the rabbits were anesthetized *via* intravenous injection of pentobarbital and their abdominal hair was shaved off, the abdomens were opened to expose the liver. A "+" shaped wound approximately 2×2 cm with the depth of 3 cm was formed using a scalpel. Approximately 5 g of 6MS or 6CaMS granules were directly sprinkled on top of the bleeding liver and covered with a pad of gauze. Manual compression on the wound site was applied. The gauze was slightly uplifted to observe the bleeding every five seconds until the bleeding stopped, and then the superficial samples were wiped from the injury site. Samples after hemostasis were collected for SEM observation to explore the interaction between the sample and the blood. After completion of the treatment, the abdomen was temporarily closed with a monofilament suture, and the animal was monitored for 180 min after injury or until death, whichever came first.

2) Rabbit femoral artery injury experiment

15 rabbits separated into three groups (6MS, 6CaMS and Standard gauze) were anesthetized, and their hair was shaved off to expose the groin with their hind limbs extended. After transecting the femoral skin and overlying muscles, the femoral artery was exposed and a massive hemorrhage was created by clipping the femoral artery. Immediately, approximately 8 g of 6MS or 6CaMS were applied to the injury site. Manual compression on the wound site was needed and given by a pad of gauze until the bleeding ceased. The gauze was slightly uplifted to observe the injury condition every five seconds. At the end of the study period, each groin was opened and both the liquid and clotted inguinal blood and materials were suctioned and measured. To further evaluate the effect of hemostasis, the mortality rate for the femoral artery injury was calculated by division of the amount of the dead rabbit by the total amount of rabbits within 2 h after hemostasis. After being supervised for 2 h, the surviving rabbits were euthanized using an overdose of pentobarbital.

75 Statistical analysis

Results were expressed as means \pm standard deviations. Except special requests in the animal experiment, all data were generated using more than three independent experiments. Statistical analysis was conducted using one-way analysis of variance (ANOVA). A value of $P < 0.05$ was considered to be statistically significant.

Results and discussion

Chemical modification is such an effective method to generate different surface properties. Protein adsorption is essential in the blood-borne hemostatic response of foreign materials. In an initial response, during blood-material contact, protein adsorption mechanism is greatly affected by the surface properties of the material. It was reported that platelets adhered to positively charged surfaces,²⁹ and negatively charged surfaces induced coagulation initiated *via* the auto-activation of coagulation factor XII.³⁰ Therefore, chemically modified MS, an active hemostatic agent, could enhance the hemostatic capacity not only by its physical adsorption but also by activating platelets. However, these modified MSs showed poor degradability or toxicity after modifications.²³

The calcium ions (the fourth clotting factor) are important to activate the coagulation system to form thrombin, a key enzyme in the "waterfall reaction" of blood clotting, to support earlier fibrin generation.³¹⁻³² Additionally, intracellular Ca^{2+} can cause phosphatidylserines to be exposed to the platelet surface, which provides more locations for assembling coagulation complexes and amplifies the formation of thrombin. Then, the thrombin further induces the aggregation of platelets and the release of tissue factors to create a positive feedback loop.³³⁻³⁴ Ca^{2+} can also increase the clot rigidity, which is beneficial to stop bleeding.³⁵ Therefore, in this study, an alternative CaMS hemostatic agent was developed by chemically modifying Ca^{2+} on MS to introduce the active hemostatic mechanism.

Characterization of the prepared CaMS

The functional group on starch that readily targetable for chemical modifications is only the glucose free hydroxyl group. However, our preliminary experiments showed that Ca^{2+} was difficult to react with the hydroxyl groups. Ca^{2+} could be loaded into MSs only by physical adsorption, but the amount of calcium absorbed was low and it was labile to be washed away by the blood. Therefore, how to modify Ca^{2+} effectively onto MSs was still a challenge.

In the past decade, large amounts of Ca^{2+} in industrial effluents have been removed by oxidized starch because of the strong chelation interaction between carboxyl groups and metal ions.³⁶⁻³⁷ Interestingly, it was reported that hydrophilic carboxyl groups trigger the contacting activation of the blood,³⁸⁻³⁹ and oxidized starch showed better degradability than normal starch⁴⁰. Thus, in this study, we introduced carboxyl groups onto MS and combined them with Ca^{2+} by exploiting the chelating properties of oxidized starch. Subsequently, the hemostatic efficiency and degradability of the modified MS have been improved greatly with the synergistic effect of passive and active mechanisms.

An inspiration obtained from the adsorption of Ca^{2+} to oxidized starch gave us the direction to introduce carboxyl groups in MS. In this study, the chemical structures of 6MS and 6OMS are characterized by FTIR in Fig. 2a. The characteristic absorption band at 1721.3 cm^{-1} on 6OMS was associated with the carboxyl group. FTIR indicated that the carboxyl groups had been

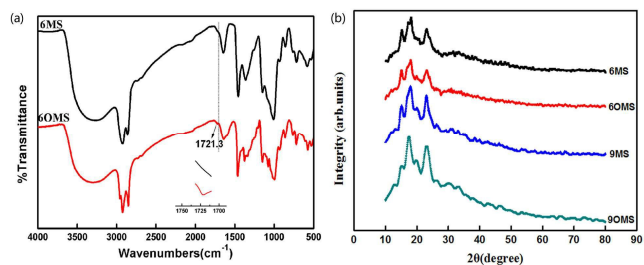


Fig. 2. (a) FTIR spectra of 6MS and 6OMS. (b) XRD patterns of 6MS, 6OMS, 9MS and 9OMS.

successfully introduced to 6MS by oxidation of hydroxyl groups after hydrolysis of starch. The oxidation process did not disrupt the ordered structures of crystalline region in 6OMS and 9OMS (Fig. 2b). Titration results presented show that each gram of 6CaMS or 9CaMS respectively contains about 0.085 mmol or 0.068 mmol carboxyl groups. ICP showed that each gram of 6CaMS and 9CaMS contained $2.8 \pm 0.28\text{ mg}$ and $2.5 \pm 0.25\text{ mg}$ of Ca^{2+} , respectively.

XRD patterns of MS and OMS are shown in Fig. 2b. It was evident that the native corn starch had four characteristic peaks at 14.94° , 17.08° , 17.74° and 22.94° , which are typical of an A-type starch structure. The crystallinity of 9MS was higher than 6MS. Amorphous regions of MS were time-independently decreased after hydrolysis and oxidation. This indicated that the amorphous parts were easily destroyed by external forces, and the enzymolysis reaction mainly occurred in the amorphous regions of the starch⁴¹. There was almost no difference in crystallinity between MS and OMS. The result indicated that oxidation did not disrupt the ordered structure of the crystalline regions in 6OMS and 9OMS.

The CaMS starch was successfully fabricated by utilizing the strong chelation between carboxyl groups and Ca^{2+} . Fig. 3 illustrates the SEM micrographs of MS and CaMS. It clearly showed that there were many spherical-shaped microspores on the surface. The pore size of 9MS (Fig. 3c) was larger than that of 6MS (Fig. 3a) and a helix path of hydrolysis was more obvious in Fig. 3c, indicating that the depth of microspores increased with increasing hydrolysis time. Compared with 6MS and 9MS, 6CaMS (Fig. 3b) and 9CaMS (Fig. 3d) displayed larger apertures and increased surface roughness respectively, which was attributed to surface erosion resulting from the oxidation treatment. However, some microspores in 9CaMS were destroyed and starch microspheres were partially collapsed to debris after oxidation.

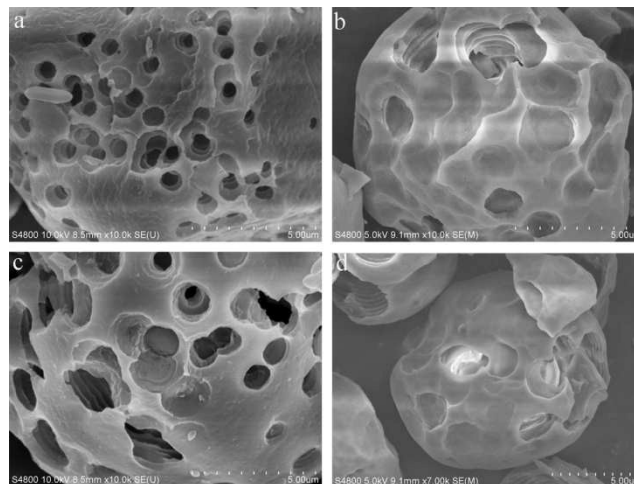


Fig. 3. SEM micrographs of (a) 6MS, (b) 6CaMS, (c) 9MS and (d) 9CaMS.

6.5 Degradation, absorption ratio, solubility and swelling *in vitro*

Degradation is an important quality for a hemostatic destined to be used *in vivo*. It is well known that non-degradable hemostasis agents that remains in the body may incite an inflammatory reaction and impair mucosal regeneration. Furthermore, non-degradable hemostatics tend to cause re-bleeding during the removal. Fig. 4a displays the weight loss of MS and CaMS against the immersion time. The degradation rate of all samples increased with time after immersion. The weight loss of the samples was the greatest during the first two days of immersion. Shortly thereafter weight loss plateaued. Interestingly, although

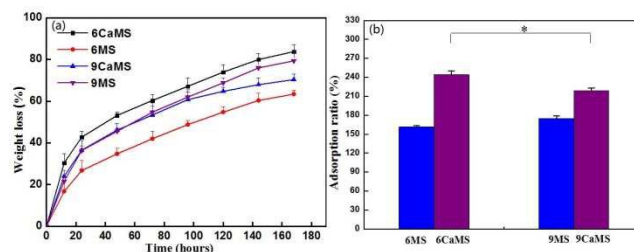


Fig. 4. (a) Weight loss curves of samples against immersion time in mSBF. (b) Absorption ratio of samples in mSBF, * $P < 0.05$. Data are represented as mean \pm SD ($n = 3$).

there was no significant difference between 9MS and 9CaMS in weight loss during the first five days, 9MS (76%) had a higher weight loss than that of 9CaMS (68%) on the sixth immersion day. After immersion for 7 days, the 6CaMS possessed the greatest weight loss of 83.8%, while 6MS showed the lowest weight loss of 63.4%. This may be due to the porous structure of the MS, the oxidation treatment, and the self-assembling of calcium ions on the starch.

Fig. 4b shows the absorption ratio of MS and CaMS in mSBF. The absorption ratio of CaMS was much higher than that of MS at the same hydrolysis time. 6CaMS had the highest absorption of 244.2%, nearly 50% higher than that of 6MS (161.5%). The absorption of 9CaMS and 9MS were 175.2% and 219.1%, respectively. 6CaMS exhibited a higher absorption than 9CaMS. This may be due to the reduced surface area caused by structure collapse due to excessive oxidation.

Tab.1 plots the physical properties of corn starch, 6MS and 6CaMS. It was obvious that 6CaMS had the highest solubility, swelling and absorption ratio, which was conducive to improving the efficacy in controlling bleeding. The result indicated that chemical modification is an effective method to increase hemostatic activity of the starch particles.

Due to the higher degradation and absorption *in vitro* of 6CaMS than 9CaMS, only 6CaMS, 6MS and control group were used in the following experiment.

APTT and PT assay

Hemostasis is a finely tuned process that prevents significant blood loss following vascular injury⁴². This process depends on an intricate series of events involving platelets, other cells and the activation of specific blood proteins known as coagulation factors. Therefore, in this work, prior to the *in vivo* experiment, *in vitro* activated partial thromboplastin time, prothrombin time, and platelet adhesion were carried out. PTs and APTTs of samples were determined and the results are presented in Fig. 5. Compared with the control (standard gauze), the APTT of 6MS was higher than 6CaMS. When the amount of 6CaMS increased from 2 mg to 4 mg, the APTT of 6CaMS dropped to approximately half of its initial value (Fig. 5(a)). In addition, Fig. 5 (b) shows that the PTs of samples follow a similar trend to that seen in the APTT, with 6CaMS shortening PT more than 6MS. However, there had no significant dosage-dependent relationship observed in PT since it did not change obviously with the use of 4 mg of sample compared to the 2 mg samples. The results indicated that the prepared CaMS could not only shorten the time of initial fibrin formation significantly, but also accelerate the activation of the intrinsic coagulation system. With an increase in CaMS content, its coagulation system activation effects became obvious.

Platelet adhesion

Platelet adhesion to the samples was evaluated by agitation of the samples in PRP followed by image capture of samples with adherent platelets by SEM (Fig. 6). It can be seen that the number of platelets adhered to the 6CaMS increased greatly. Although there was no statistically significant differences between Control group and 6MS in platelet number, statistically significant differences ($p < 0.05$) were found between 6CaMS and 6MS or

Table 1 The physical properties of corn starch, 6MS and 6CaMS

	Corn starch	6MS	6CaMS
Solubility (%)	0.21	8.01	11.71
Swelling (%)	153.74	398.32	420.42
Absorption ratio (%)	56.3	161.5	244.2

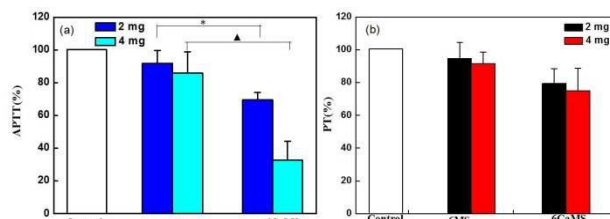


Fig.5. Influence of samples on the activated partial thromboplastin time (APTT) and prothrombin time (PT) of rat plasma (a) APTT. (b) PT. “%” represents the ratio against control group.

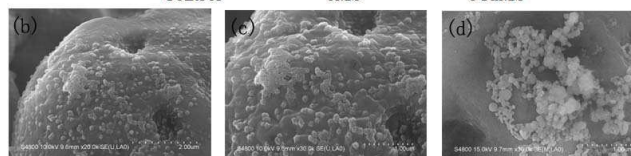
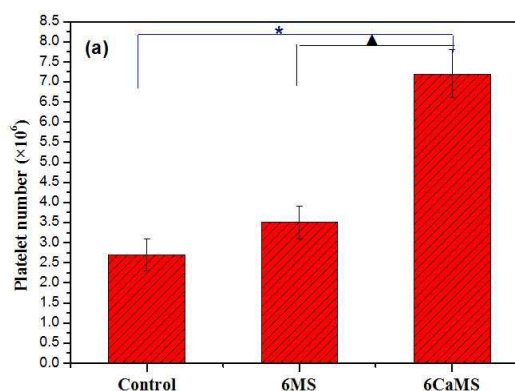


Fig.6. (a) Platelet adhesion to the materials after cultured for 30 min. SEM images of platelets adhered to the surface of (b) CaMS, (c) high-magnification image of (b) and (d) MS. * and ▲ both indicate significant difference, $p < 0.05$.

Control group. SEM images presented the morphology of adhered platelets after 30 min exposure of materials to PRP. The surfaces of 6MS and 6CaMS were both covered with numerous adhered platelets. However, it can be observed that platelet aggregation was stimulated by 6CaMS while platelets on the surface of 6MS were arranged more scattered. The result showed that Ca^{2+} in CaMS promoted the aggression and activation of platelets.

Hemostasis in rabbit liver and femoral artery injury

The liver injury of rabbits was surgically induced as described above, and treated with MS, CaMS or standard gauze (Fig. 7). The time to complete hemostasis in different groups was recorded. After 50.5 ± 7.6 s (MS group, $n = 5$), 23.3 ± 6.2 s (6CaMS group, $n = 5$), complete hemostasis was achieved. However, in the controls ($n = 5$), a prolonged time of 362.3 ± 21.7 s was needed for

complete hemostasis.

Statistically significant differences ($p < 0.05$) were all found among the control, 6MS and 6CaMS groups. These results indicate that our microporous starch preparations (both MS and CaMS) were effective at inducing complete hemostasis in induced liver injuries. Furthermore, the hemostasis time for the CaMS groups was shorter than for the MS groups, with 6CaMS displaying superior hemostatic performance (least time to hemostasis) in liver injury.

Fig. 8 shows the treatment process for rabbit femoral artery injury. Robust clots were formed with the samples, platelets, and clotting proteins tightly adhering to the bleeding surface. The time to complete hemostasis was recorded. After 62.5 ± 7.5 s (6CaMS group, $n = 5$), 116.7 ± 9.4 s (6MS group, $n = 5$), complete hemostasis were achieved. No matter how much pressure applied, the injuries in control group ($n = 5$) were always continuous bleeding and the hemostasis could not be controlled effectively. In the control group, the femoral artery injury resulted in 100% mortality. However, the application of CaMS and MS both decreased the mortality rate to 0 % within 2 h after hemostasis significantly. Statistically significant differences ($p < 0.05$) were found between the control group and 6MS group or 6CaMS group.

All these showed that CaMS could effectively control the bleeding, and 6CaMS showed the best hemostatic performance.

Fig. 9 reveals the SEM morphologies of 6MS and 6CaMS interacting with the blood. It can be observed that a number of blood cells were closely agglutinated on 6MS and 6CaMS. Furthermore, many fibrins in a mesh structure were found on 6CaMS, and closely bound to the blood cells around starch microspheres.

Hemostatic mechanism

Although the exact hemostatic mechanism for these new CaMS was not clear, the mechanisms of their action can be explained through some of the observations. On one hand, the mechanism of the action of CaMS can be associated with the adsorption of water. Being a starch, both the CaMS and MS prepared here possess a large number of hydrophilic hydroxyl groups, which result in a high adsorption capacity. The porous structure and high surface area produced by enzymatic hydrolysis further enhanced the water absorption of CaMS and MS (Fig. 3). Generally speaking, the adsorption capacity is positive correlated to the surface area. The oxidation reaction and modification process further yet increased the pore size of the CaMS, as well as increased its surface area, giving the CaMS a higher water adsorption than MS (Fig. 4). Upon contact with blood or other wound exudates, the CaMS particles act as a molecular sieve to rapidly dehydrate blood and concentrate blood solids such as platelets and red blood cells to accelerate the clotting cascade, and thus helping to quickly form blood clots at the site of the wound. SEM photographs (Fig.9) revealed the formation of the fibrin matrix after the material was exposed to the whole blood.

Conversely, the hemostatic mechanism of CaMS depends primarily on the Ca^{2+} that is released from the material into the blood at the site of injury. Blood coagulation is a complex biochemical process involving platelets and dozens of proteins. The activation of platelets triggers a multistep cascade that

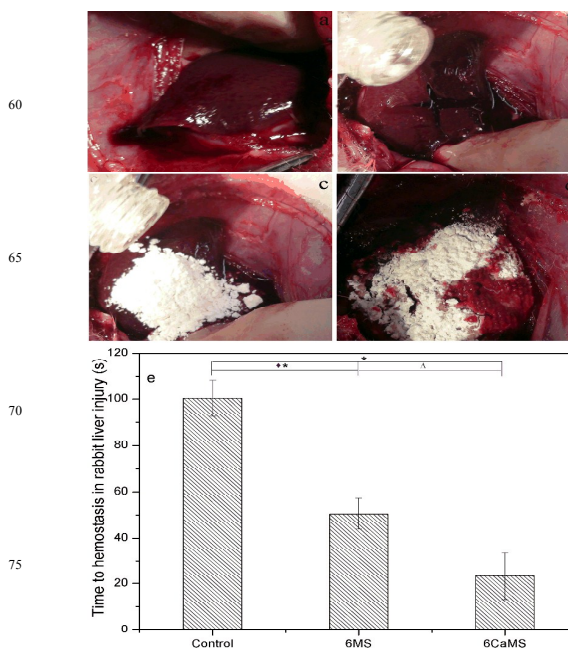


Fig. 7. Hemostasis in rabbit liver injury. (a) Expose the liver, (b) A "+" shaped wound was created leading to blood loss, (c) Samples were applied to the injury sites, (d) Complete hemostasis was achieved and a clot formed at the site of injury, (e) Hemostatic time in rabbit liver injury. *, ** and Δ all indicate significant difference, $p < 0.05$.

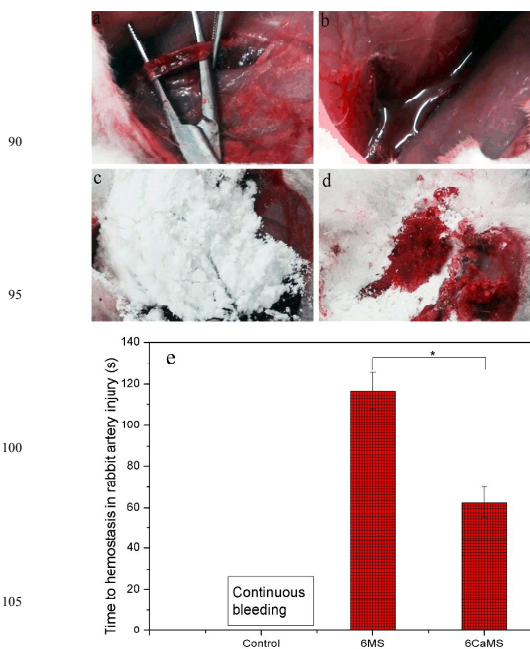


Fig. 8. Hemostasis in rabbit artery injury. (a) Expose the femoral artery; (b) Cut the artery leading to blood loss; (c) Pouring samples into the injury site immediately; (d) Complete hemostasis was achieved after slight pressure was offered over the wound. Note that the clots formed tightly adhered to the wound and bleeding completely ceased; (e) Hemostatic time in rabbit artery injury. * indicates significant difference, $p < 0.05$.

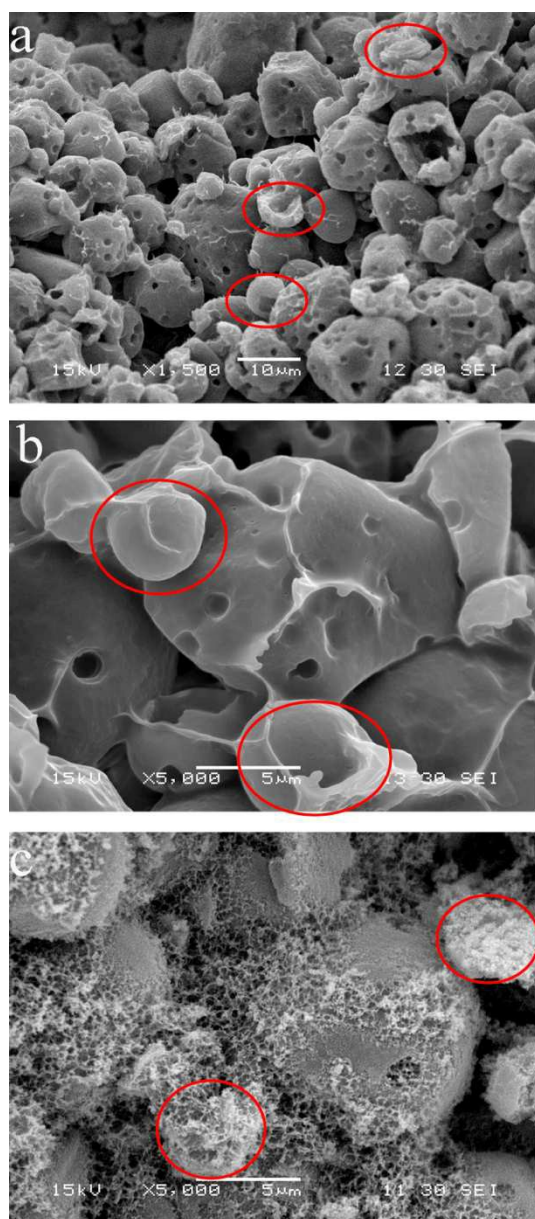


Fig. 9. SEM images of (a) 6MS \times 1500, (b) 6MS \times 5000 and (c) 6CaMS \times 5000 after hemostasis. Many fibrins were found to gather on the surface of 6CaMS. Blood cells are signified by red circles.

produces a clot. Calcium, acting as Factor IV, is involved at several steps in this cascade. With the help of calcium ions, hemostatic mediators are secreted from thrombocytes.⁴³ It activates thrombocytes, Factor VII-IX and X in hemostasis. In addition, calcium ions mediate the binding of the tenase and prothrombinase complexes to exposed phospholipids surfaces expressed by platelets as well as procoagulant microparticles or microvesicles shed from them and are required for stable platelet incorporation into the thrombus⁴⁴. Furthermore, calcium ions help to maintain the heterodimeric structure of fibrinogen receptor GP II b/IIIa, which is the most abundant receptor on the platelet surface with about 50,000 integrins per platelet. As expected, we could clearly see that CaMS activated more platelets and

20 adsorbed a greater amount of platelets adhering on their surfaces. The results of the PT and APTT (Fig. 7- Fig. 8) also reflected the acceleration of activation of intrinsic pathway by CaMS. In turn, the increase of the local concentration of platelets, blood coagulation factors, and fibrin initiate and enhance the internal clotting mechanism.

Platelets adhere, activate, and aggregate at the broken surfaces, acting as the first response to attempt to stop the bleeding by rapidly forming a platelet plug of aggregated platelets. In addition to Ca^{2+} , the carboxyl groups introduced onto the oxidized starch were found to induce platelet adhesion. To stabilize the platelet plug and further seal up the wound, it is necessary for the platelets to activate and amplify the coagulation cascade process. Some authors demonstrate that the stability of the clot is affected by the structure of the fibrin formations, and increased levels of thrombin will generate finer fibrin networks which are more resistant to fibrinolysis⁴⁵. After the hemostasis, we found that the clots produced by 6CaMS were robust and could not be broken by touching with tweezers. However, the clots produced by 6MS were loose and broken easily. Therefore, compared with MS, CaMS produced more stable hemostatic clots when they adhered to the wound. In addition, many fibrins were found to gather on the surface of 6CaMS. Furthermore, applying pressure during the animal experiment helped to form a tight contact. CaMS and the bleeding surface. The resultant compression of capillaries allows for platelet aggregation and thrombus formation. Furthermore, when CaMS dehydrated the blood, the subsequently compacted cells also assisted in activating the clotting process. This is also the possible explanation for the low re-bleed rate of CaMS. Therefore, the calcium ions in CaMS had greatly improved the material's hemostatic properties. Based on the above analysis, we elaborated a combination hemostatic mechanism model of CaMS, as shown in Fig. 10.

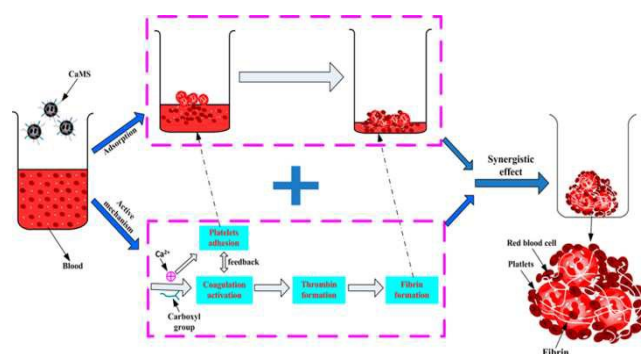


Fig. 10. Schematic diagram of the CaMS hemostatic process with a combination of physical (adsorption) and chemical (activation the coagulation cascade) mechanisms.

Conclusions

CaMS has been successfully developed to control hemorrhaging, and its hemostatic efficacy together with degradable properties were evaluated. The results showed CaMS could not only activate the intrinsic coagulation cascade pathway and induce platelet

adherence by modifying with calcium ions and carboxyl groups, but also promote water absorption due to the starch's porous structure and high surface area. The synergistic effects of chemical activation and physical absorption endowed CaMS potent hemostatic properties. CaMS showed a high degradability. The fabricated CaMS, with a combination of improved hemostatic efficiency and excellent degradability, should be a strong candidate for controlling hemorrhaging. Research is ongoing to explore the molecular mechanism of their hemostatic activity and explore other chemical modifications to enhance the hemostatic efficiency of MS. Additionally, although the hemostatic efficacy of CaMS was verified in rabbit liver and femoral artery injuries, more serious injury models in larger animals such as in a lethal swine groin injury should be tested with this device in the future.

Acknowledgements

This investigation was supported by the National Basic Research Program of China (973 Program : 2012CB933600), National Natural Science Foundation of China (No.31370960, No. 31100678), National Science & Technology Pillar Program during the Twelfth Five-years Plan Period (No.2012BAD32B01) and Program of Shanghai Leading Academic Discipline Project (No. B502).

Notes and references

- [1] C.N. Sambasivan, D. Cho, K.A. Zink, J.A. Differding and M.A. Schreiber, *Am. J. Surg.*, 2008, **197**, 576-80.
- [2] J.F. Kelly, A.E. Ritenour, D.F. McLaughlin, K.A. Bagg, A.N. Apodaca and C.T. Mallak, *J. Trauma*, 2008, **64**, S21-6.
- [3] C.L. Dai, Y. Yuan, C.S. Liu, J. Wei, H. Hong and X.S. Li, *Biomaterials*, 2009, **30**, 5364-75
- [4] M.C. Neuffer, J. McDivitt, D. Rose, K. King, C.C. Cloonan and J.S. Vayer, *Mil. Med.*, 2004, **169**, 716-20.
- [5] C.L. Dai, C.S. Liu, J. Wei, H. Hong and Q.H. Zhao, *Biomaterials*, 2010, **31**, 7620-30
- [6] A.E. Pusateri, J.B. Holcomb and B.S. Kheirabadi, *J. Trauma*, 2006, **60**, 674-82.
- [7] K.R. Ward, M.H. Tiba, W.H. Holbert, C.R. Blocher, G.T. Draucker and E.K. Proffitt, *Trauma*, 2007, **63**, 276-84.
- [8] B.S. Kheirabadi, J.W. Edens, R. Terrazas, J.S. Estep, H.G. Klemcke and M.A. Dubick, *Trauma*, 2009, **66**, 316-26.
- [9] F. Arnaud, K. Teranishi, T. Okada, S.D. Parreño, D. Hupalo and G. McNamee, *J. Surg. Res.*, 2011, **169**, 92-8.
- [10] B.S. Kheirabadi, E.M. Acheson, R. Deguzman, J.L. Sondeen, K.L. Ryan and A. Delgado, *J. Trauma*, 2005, **59**, 25-35.
- [11] T. Peng, *Trends. Biomater. Artif. Organs.*, 2010, **24(1)**, 27-68.
- [12] J.K. Wright, J. Kalns, E.A. Wolf, F. Traweek, S. Schwarz and C.K. Loeffler, *J. Trauma*, 2004, **57**, 224-30.
- [13] A. Meer Tarique, F. Ritesh, S. Ajay and A. Purnima, *AAPS. Pharm. Sci. Tech.* 2013, **14(3)**, 919-926
- [14] L.M. Che, D. Li, L.J. Wang, N. Özkan, X.D. Chen and Z.H. Mao, *Int. J. Food Prop.*, 2007, **10 (4)**, 911-22
- [15] J.L. Antisdell, J.L. West-Denning, R. Sindwani and S. Louis, *Otolaryng. Head. Neck.*, 2009; **141**: 353-7
- [16] R. Sindwani and S. Louis, *Otolaryng. Head. Neck.*, 2009, **140**, 262-3.
- [17] K. Björse and J. Holst, *Eur. J. Vasc. Endovasc. Surg.*, 2007, **33**, 363-70.
- [18] H.B. Alam, G.B. UY, D. Miller, E. Koustova, T. Hancock and R. Inocencio, *J. Trauma.*, 2003, **54**, 1077-82.
- [19] M.L. Biondo-Simoes, R. Petrauskas, A.G. Dobrowolski, G. Godoy, F. Kaiber and S.O. Ioshii, *Acta. Cir. Bras.*, 2007, **22(1)**, 29-33.
- [20] M.C. Neuffer, J. McDivitt, D. Rose, K. King, C.C. Cloonan and J.S. Vayer, *Mil. Med.*, 2004, **169(9)**, 716-20.
- [21] K. Björse and J. Holst, *J. Trauma*, 2009, **66(3)**, 602-11.
- [22] S. Samudrala, *Aorn. J.*, 2008, **88**, S2-11.
- [23] K. Björse, L. Faxalv, C. Montan, K. Wildt-Persson, P. Fyhr and J. Holst, *Acta. Biomater.* 2011, **7**, 2558-65.
- [24] M.R. Humphrey, E.P. Castle, P.E. Andrew, M.T. Gettman and M.H. Ereth, *Am. J. Surg.*, 2008, **195**, 99-103.
- [25] M. Kabiri, S.H. Emami, M. Rafinia and M. Tahriri, *Curr. Appl. Phys.* 2011, **11**, 457-61.
- [26] O.D. Ratnoff and A.M. Potts, *J. Clin. Invest.*, 1954, **33**, 206-10.
- [27] T. Kokubo, *J. Non-Cryst. Solids*, 1990, **120**, 138-51.
- [28] S.Y. Ong, J. Wu, S.M. Mochhala, M.H. Tan and J. Lu, *Biomaterials*, 2008, **29**, 4323-32.
- [29] S. Dhital, A. K. Shrestha, M. J. Gidley, *Food Hydrocolloids* 2010, **24**, 152-163
- [30] C. Sperling, M. Fischer, M.F. Maitz and C. Werner, *Biomaterials*, 2009, **30(27)**, 4447-56.
- [31] S. Sarkar, K.M. Sales, G. Hamilton and A.M. Seifalian, *J. Biomed. Mater. Res. B: Appl. Biomater.*, 2007, **82(1)**, 100-8.
- [32] M.B. Gorbet and M.V. Sefton, *Biomaterial*, 2004, **25**, 5681-703.
- [33] X. Chen, J. Wang, Z. Paszti, F.L. Wang, J.N. Schrauben and V.V. Tarabara, *OAnal. Bioanal. Chem.*, 2007, **388**, 65-72.
- [34] M.T. Harper and A.W. Poole, *Cell. Calcium.*, 2011, **50**, 351-8.
- [35] D.M. Monroe and M. Hoffmann, *Arterioscl. Throm. V.*, 2006, **26**, 41-84.
- [36] L.L. Shen, J. Hermans, J. McDonagh and R.P. McDonagh, *Thromb. Res.*, 1975, **6**, 255-65.
- [37] Y.X. Chen and G.Y. Wang, *Colloid. Surface A.*, 2006, **289**, 75-83.
- [38] D.K. Kweon, J.K. Choi, E.K. Kim and S.T. Lim, *Carbohydr. Polym.*, 2001, **46**, 171-7.
- [39] Z. Guo, K.M. Bussard, K. Chatterjee, R. Miller, E.A. Vogler and C.A. Siedlecki, *Biomaterials*, 2006, **27**, 796-806.
- [40] C. Sperling, M. Fischer, M.F. Maitz, C. Werner, *Biomaterials*, 2009, **30**, 4447-56.
- [41] H.J. Chung, D.H. Shin and S.T. Lim, *Food. Res. Int.*, 2008, **41**, 579-85.
- [42] H. Jacobs and J.A. Delcour, *J. Agric. Food. Chem.*, 1998, **46**, 2895-905.
- [43] R.W. Colman, A.W. Clowes and J.N. George, 5th edn. Colman RW, Clowes AW, George JN et al. (editors). Philadelphia: Lippincott, Williams & Wilkins, 2006, 1-16.
- [44] T. Ali Kemal, Y. Mehmet, Ö. İsmet, K. Bülent, B. Orhan and A. Seyit, *J. Trauma & Emerg. Surg.*, 2013, **19 (3)**, 195-9.
- [45] T.J. Kunicki, D. Pidad, J.P. Rosa and A.T. Nurden, *Blood*, 1981, **58**, 268-78.
- [46] A.S. Wolberg and R.A. Campbell, *Transfus. Apher. Sci.*, 2008, **38**, 15-23.

[47] H. B Alam, G. B. Uy, D. Miller, E. Koustova, T. Hancock, R. Inocencio, D. Anderson, O. Llorente and P.Rhee, *J. Trauma.*, 2003, **54**, 1077–82